Iran Polym J (2015) 24:651–661
DOI 10.1007/s13726-015-0354-z

ORIGINAL PAPER

Synthesis and characterisation of poly(epichlorohydrin-*g*-Fe_3O_4/congo red)-*co*-poly(methylmethacrylate)

S. Luna Eunice[1] · B. Meenarathi[2] · S. Palanikumar[2] · R. Anbarasan[2]

Received: 22 December 2014 / Accepted: 13 June 2015 / Published online: 23 June 2015

Abstract A magnetic and fluorescent copolymer nanocomposite was prepared and characterized by various analytical techniques. Poly(epichlorohydrin) (PECH) was prepared by solution polymerization method using methacrylic acid as a chemical initiator and its copolymer was prepared by emulsion polymerization. After the structural modification of the copolymer with a nanohybrid system, its thermal properties were improved. The nanohybrid system consisting of Congo red dye decorated ferrite nanoparticles was synthesized by the conventional method and characterized by UV–Visible, fluorescence emission and excitation spectroscopy methods, high resolution transmission electron microscopy, and vibrating sample magnetometer techniques. Due to the decoration and encapsulation phenomena, the magnetic moment value of Fe_3O_4 was found to be decreased. While increasing the loading of nanohybrid system, the glass transition temperature (T_g) of poly(methylmethacrylate) was increased. The TGA study inferred that by increasing the loading of nanohybrid system, the percentage weight residue remained above 550 °C was also increased. The chemical grafting of nanohybrid system onto the PECH-based copolymer backbone was confirmed by NMR spectroscopy and GPC analysis. The weight average molecular weight (M_w) of the copolymer and nanohybrid-grafted copolymer exhibited higher M_w than that of the PECH homopolymer. In the present study, we simply prepared a novel material and characterized it by various analytical methods.

Keywords Copolymer · Synthesis · Characterization · Nanocomposite · Nanohybrid · Ferrite nanoparticles

Introduction

Synthesis of novel bio-degradable and bio-compatible polymeric materials with improved physical, chemical, and biological properties has become an attractive field in polymer science and technology. Structural modification or copolymerization of the existing polymers is one of the ways to improve the properties of polymeric materials. It combines the best characteristics of the constituents toward certain end use application.

Polyethers such as poly (epichlorohydrin) (PECH) has wide range of applications, e.g., in drug delivery systems [1] and ionic conductive polymers in batteries [2]. PECH can be synthesized with the help of rare earth catalytic systems [3]. Epichlorohydrin (ECH) and ethylene sulfide copolymer was prepared for photoelectrochemical cells [4]. ECH-based copolymer was synthesized for bio-metallic ion channels [5]. There are also other works about the structural modification and copolymerisation of ECH by mesogenic acids [6], flavanoids [7], PVA [8], surfactant [9], and carboxylates [10].

Poly(methylmethacrylate) (PMMA) is a well-known plastic candidate owing to its transparency and eco-friendly nature. Various methodologies are adopted for synthesis of PMMA such as click chemistry [11], dispersion [12], free radical [13], bulk [14], RAFT [15], ATRP [16], anionic

Electronic supplementary material The online version of this article (doi:10.1007/s13726-015-0354-z) contains supplementary material, which is available to authorized users.

✉ R. Anbarasan
anbu_may3@yahoo.co.in

[1] Department of Chemistry, Kamaraj College of Engineering and Technology, Virudhunagar 626 001, Tamil Nadu, India

[2] Department of Polymer Technology, Kamaraj College of Engineering and Technology, Virudhunagar 626 001, Tamil Nadu, India

[17], and suspension [18] techniques. In order to improve the physical, chemical, and bio-medical applications of PMMA, the modification methodologies were used and it was copolymerized with other conventional monomers [19, 20]. For example, Gong et al. [21] studied the ATRP of MMA in an ionic liquid. PMMA-based diblock copolymer has been reported in literature [22, 23]. Tang et al. [24] explained the PMMA-based diblock copolymer with thermo responsive property. PMMA-based triblock copolymer was synthesized by ATRP [25].

By combining MMA and ECH segments, one can get a flexible and bio-degradable polymer with –Cl pendant groups. This offers further structural modification reaction. Thorough literature survey, we could not find any report based on the ECH grafted acrylate-based copolymer. The novelty of the present investigation is the synthesis and characterisation of a stable copolymer with fluorescence and magnetic properties.

Among azo dyes, Congo red (CR) dye occupies the first place because of its wide application in medical field as a bio-imaging agent in its hybrid form [26]. After the utilization, CR dye was photodegraded by Fe_3O_4 [27] and ZnO [28]. In the bio-probe application, shorter time of photo excitation (particularly in near infrared region) is required and hence the system is an effective one. Intra vital imaging study of CR was reported by Hu et al. [29]. CR was used as an imaging agent in bio-medical field by different research teams [30, 31].

On going through the literature, we could not find any report based on CR/Fe_3O_4 nanohybrid system and CR-grafted PECH copolymer. By way of structural modification of PECH, the bio-medical value can be increased. The purpose of using dye is to increase its application as a bio-probe in the bio-medical field. The applications of ferrite nanoparticles are increased in the bio-medical field as a targeted drug delivery material [32]. The combination of targeted fluorescent material as a bio-probe urged us to do the present investigation. Moreover, in this study we have prepared and characterized a fluorescent material. The novelty of the present investigation is the synthesis and characterization of the fluorescent and magnetic nanocomposite without sacrificing the properties of PMMA. For example, the molecular weight and thermal properties were increased. The main aim of the present investigation is just the preparation of a material for bio-imaging application.

Experimental

Materials

Phthalic anhydride (PAH), peroxy disulfate (PDS),Congo red dye (CR), sodium lauryl sulfate (SLS), ferric chloride ($FeCl_3$), ferrous sulphate ($FeSO_4$), and sodium hydroxide (NaOH) pellet were purchased from Nice Chemicals Co., India. All of the materials and methacrylic acid (MA, Aldrich, USA), Epichlorohydrin (ECH, Aldrich, USA), and methylmethacrylate (MMA, CDH, India) were used without any further purification. Double-distilled (DD) water was used for making solutions. Tetrahydrofuran (THF, CDH) was used as a solvent for dissolution of polymer.

Method

Synthesis of Fe_3O_4/CR nanohybrid system

One gram CR dye was dissolved in 50 mL of DD water under ultrasonication, and then put in a 500 mL beaker with vigorous stirring. Amounts of 2.5 g $FeSO_4$ and 5 g $FeCl_3$ were added into the beaker under N_2 atmosphere at room temperature. Further, 100 mL of DD water was added to increase the dissolution process quality. The mixing was continued for 10 min. Ten gram NaOH in 100 mL DD water was prepared separately, and the prepared NaOH solution was added to the beaker immediately under stirring condition till the attainment of alkaline pH (pH 10.5) [33]. Once the permanent dark color was obtained, further addition of NaOH solution was ended. The reaction was allowed to stir for further 2 h. The added NaOH nucleated the formation of Fe_3O_4. The excess NaOH was removed from the medium by placing the beaker on a magnetic bar. Under the influence of magnetic field, the CR functionalized Fe_3O_4 molecules were settled down, whereas the unreacted NaOH was still presented in the aqueous medium. The supernatant liquid was removed by a pipette. The precipitate was washed with excess amount of DD water for three times. The washing process was continued till the pH of the supernatant liquid attained pH 7.0. Finally, the precipitate was freeze dried, weighed, and stored in a zipper lock cover (Scheme 1).

Synthesis of copolymer

The present investigation includes a three-step synthesis process. In the first step, poly (epichlorohydrin) (PECH) was synthesized using MA as an initiator. In the second step, MA–PECH–poly(methylmethacrylate) (PMMA) was synthesized using peroxy disulphate as a free radical initiator through emulsion polymerization method. In the third step, the obtained copolymer was structurally modified by Fe_3O_4/CR nanohybrid system.

Five milli liter of ECH monomer was charged in a 50 mL two-way necked round bottomed flask (RBF). The two-way necked RBF was used for N_2 inlet and outlet, respectively. Two milli liter of MA initiator was added

Scheme 1 Synthesis route of Fe_3O_4/CR nanohybrid-grafted copolymer

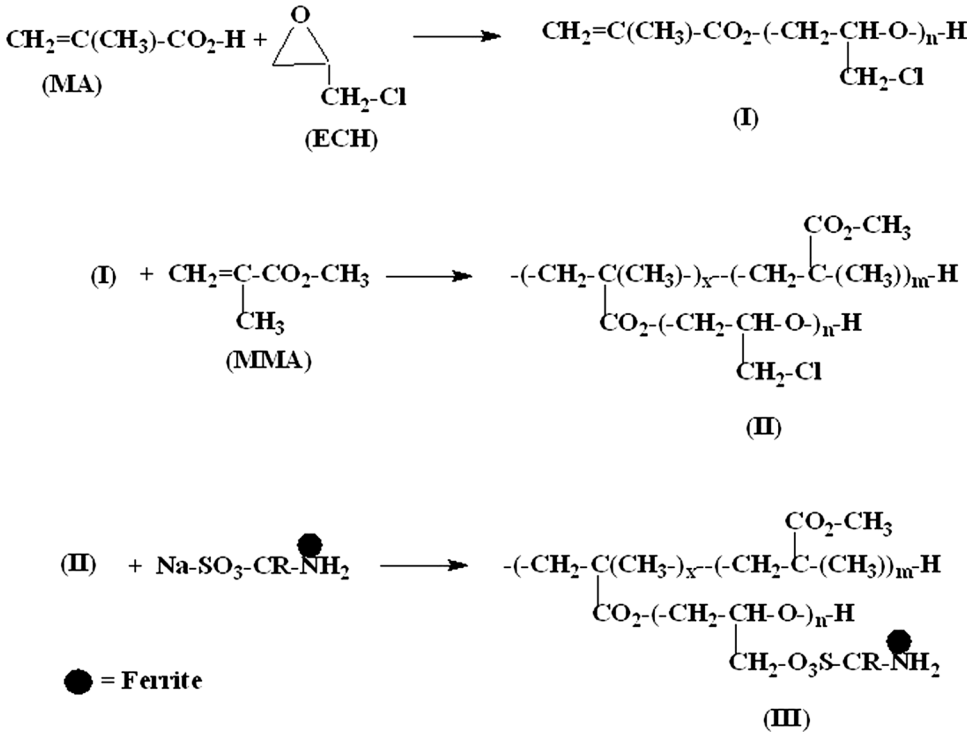

into the RBF and stirred well for 5 min. The ring opening polymerization (ROP) of ECH was induced by the addition of 0.10 g PAH as a co-monomer.

Recently, Murugesan et al. [34] reported about the PAH-assisted ROP of THF. In the present investigation, we followed the similar procedure for the synthesis of ROP of ECH. Amount of 25 mL of DD water was added and stirred well in order to get a homogeneous solution (solution polymerization method). The ROP was carried out at 45 °C for 6 h under nitrogen atmosphere with vigorous stirring. At the end of the reaction, the content was repeatedly washed with DD water. At the end of each washing, the content was evaporated to dryness at 110 °C over night. The remained water and unreacted ECH units were evaporated. Finally, PECH was obtained as a highly viscous liquid.

The copolymer consisted of ECH and MMA units was synthesized by emulsion polymerization method [35, 36]. Two g of PECH was taken in a 50 mL RBF. Five milli liter of MMA was also added into the RBF under vigorous stirring condition. Amounts of 1 g SLS and 0.50 g PDS were added under N_2 atmosphere. The system was heated at 55 °C for 4 h under vigorous stirring condition. After 4 h of stirring, the contents were thoroughly washed with 25 mL DD water for three times in order to remove the unreacted PECH or SLS. The unreacted MMA was removed by washing the product with acetone and the content was filtered and dried. Finally, the content was transferred to a petri dish for drying at 110 °C for 3 h.

Synthesis of copolymer grafted with nanohybrid system

One gram of copolymer was dissolved in 25 mL THF and transferred into a 50 mL RBF. Required amount of Fe_3O_4/CR nanohybrid system was also added and stirred well. The nanohybrid system was synthesized according to the procedure explained in our recent publication [37]. The concentration of nanohybrid system was varied between 0.10 and 0.50 g. The RBF was fitted with a Liebig condenser circulated with chilled water. Amount of 0.10 g NaOH in 5 mL DD water was added into the RBF. The system was heated at 45 °C for 6 h. During the reaction, the chlorine group of ECH unit was replaced by the amino group of CR dye with the removal of 1 mol of HCl. The amino groups of CR dye were bonded with the Fe_3O_4 surface whereas the $–SO_3Na$ groups were remained intact. The amino or imino groups of CR were interacted with –Cl groups of the copolymer in alkaline medium. The surface binding nature of the amino groups toward the Fe_3O_4 surface was well explained in our earlier publication [37]. At the end of the reaction, the content was dried at 110 °C for 2 h. Thus, the obtained dark brown colored powder as the hybrid-modified copolymer was stored in a zipper lock cover and characterized further.

Characterization

TGA analysis was performed under air purge at the heating rate of 10 °C/min using a SDT 2960 simultaneous TGA and DSC analyzer (TA instruments, USA).

Fourier transform infrared (FTIR) spectra of the samples were recorded using a Shimadzu 8400 S (Japan) instrument by KBr pelletization method in the scan range 400–4000 cm^{-1}. A sample (3 mg) was ground with 200 mg of spectral grade KBr and made into a disk under the pressure of 7 tons.

A Jasco V-570 (USA) instrument was used for UV–Visible spectroscopy measurements. A sample (2 mg) was dissolved in 10 mL of THF under ultrasonic irradiation for 10 min and subjected to UV–Visible spectroscopy measurements.

^{1}H-NMR (500 MHz) spectra were obtained using an NMR apparatus (Varian, Unity Inova-500 NMR, USA) at room temperature in deuterated DMSO solvent.

DSC was measured using Universal V4.4A TA (USA) Instruments under nitrogen atmosphere at the heating rate of 10 K/min from room temperature to 373 K. The second heating scan of the sample was considered in order to clear the previous thermal history of the sample.

A Waters 2690, U gel permeation chromatography (GPC, Germany) instrument was used to determine the M_n and M_w of the polymer samples using tetrahydrofuran (THF) as an eluent at room temperature at the flow rate of 1 mL/min against polystyrene (PS) standards.

The surface morphology of the samples was scanned by a field emission scanning electron microscopy (FESEM, JSM 6300, JEOL model, USA) instrument.

Magnetic measurements were carried out with a superconducting quantum interference device magnetometer (Lakesore-7410-VSM, USA) with magnetic fields up to 7 T at 32 °C.

Results and discussion

Charcterization of triblock copolymer

FTIR spectral analysis

Figure 1a represents the FTIR spectrum of methacrylic acid initiated ROP of ECH. The important peaks are characterized below: A broad peak around 3400 cm^{-1} is due to the –OH stretching of hydroxyl group of PECH. A twin peak around 2900 cm^{-1} is associated with the C–H symmetric (2872 cm^{-1}) and anti-symmetric stretchings (2955 cm^{-1}), respectively. The carbonyl stretching of MA unit is appeared at 1733 cm^{-1} [38]. A small hump at 1648 cm^{-1} is responsible for the C=C present in the methacrylic acid unit. The ether C–O–C linkage present in the PECH can be seen at 1033 cm^{-1}. The C–H out of plane bending vibration and C–Cl bond stretching are appeared at 738 and 611 cm^{-1}, respectively.

Figure 1b indicates the FTIR spectrum of MA–PECH–PMMA copolymer system. Here also the above said peaks

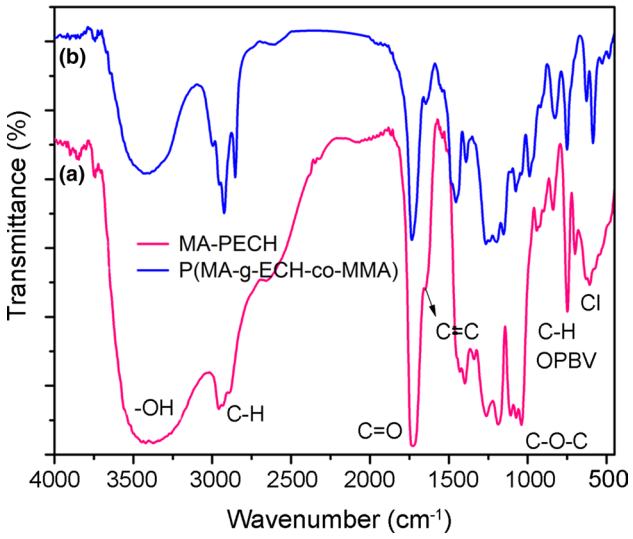

Fig. 1 FTIR spectra of *a* MA–PECH, and *b* MA–PECH–PMMA copolymer samples

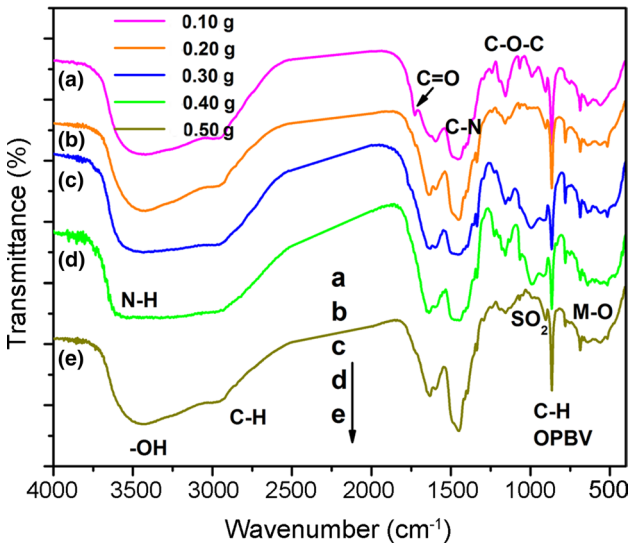

Fig. 2 FTIR spectra of MA–PECH–PMMA copolymer samples at *a* 0.10, *b* 0.20, *c* 0.30, *d* 0.40, and *e* 0.50 g loadings of Fe_3O_4/CR nanohybrid system

have appeared. The ether and ester C–O–C linkages confirmed the copolymer formation. Appearance of a small hump at 1648 cm^{-1} indicates that even after the copolymer formation traces amount of unreacted MA units were still available. This is associated with the phase separation during the copolymer preparation by an emulsion method. Above all, there is a chance for the appearance of bending vibration of water molecules.

Figure 2 reveals the FTIR spectrum of MA–ECH–PMMA–Fe_3O_4/CR system. The Fe_3O_4/CR nanohybrid

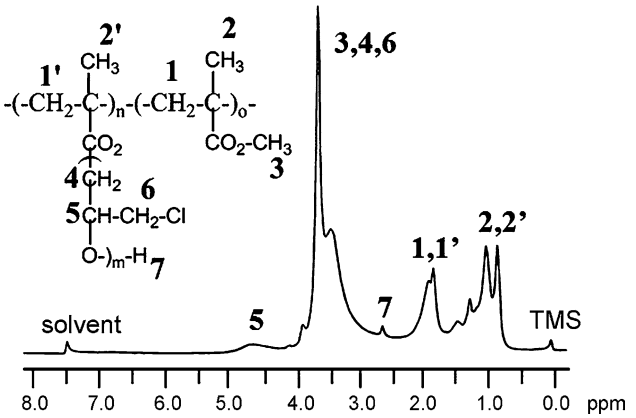

Fig. 3 ^{1}H NMR spectrum of MA–PECH–PMMA copolymer

system was loaded from 0.10 to 0.50 g. There is a change in the FTIR peaks of MA–ECH–PMMA–Fe_3O_4/CR system after loading with different concentrations of dye. A peak at 3491 cm^{-1} is due to the N–H-stretching vibration of CR dye. The C–N stretching vibration of CR dye is appeared at 1462 cm^{-1}. The $–SO_2$ stretching vibration of CR dye can be seen around 920 cm^{-1}. The $–SO_2$ stretching vibration is due to the presence of sulphonate group of CR dye. The Fe–O stretching vibration is appeared at 550 cm^{-1} [39]. Above all, the peaks appeared in the fingerprint region were varied.

The aromatic C–H out of plane bending vibration is located at 868.7 cm^{-1}. The C–Cl bond stretching vibration of PECH segments has been disappeared. The disappearance of C–Cl bond stretching vibration confirmed the existence of strong interaction between PECH unit and CR dye. The nanocomposite formation between Fe_3O_4/CR nanohybrid system and copolymer can be confirmed by the presence of a doublet peak around 560 cm^{-1}. The appearance of N–H, –C–N, $–SO_2$, and aromatic C–H out of plane bending vibrations and M–O stretching confirmed the chemical modification of copolymer by CR/ferrite nanohybrid system.

NMR analysis

The structure of copolymer was confirmed by ^{1}H NMR spectroscopy and is represented in Fig. 3. A hump at 0 ppm corresponds to TMS, an internal standard. A peak at 7.3 ppm corresponds to the solvent. A short triplet peak at 3.5 ppm is associated with the proton signals from $–CO_2Me$, $–CH_2Cl$, and $–CO_2CH_2$ moieties. The methyl protons peak from PMMA (or) MA is appeared at 1.0 ppm. The alkoxy protons peak is appeared at 4.65 ppm [38]. The methylene protons peak is appeared at 1.81 ppm. Thus, the ^{1}H NMR spectrum confirmed the chemical structure of the copolymer.

UV–Visible and fluorescence spectral analysis

The UV–Visible spectrum of pristine CR dye is shown as spectrum a in Fig. S1. The spectrum shows one sharp peak at 519 nm and one another at 430 nm corresponding to the monomeric and dimeric structures of CR dye. The fluorescence emission spectrum of pristine CR dye is given as spectrum b in Fig. S1. The spectrum shows an emission peak at 513 nm. The fluorescence excitation spectrum (excited at 358 nm) of CR dye is shown as spectrum c in Fig. S1. After nanohybrid formation, its UV–Visible spectrum exhibited an absorbance peak at 503.3 nm corresponding to the monomeric structure of CR dye (Fig. S2, spectrum a). The blue shift in the spectrum is associated with the surface functionalization reaction. This can also be explained on the basis of decrease in the conjugation length or resonance stabilization of CR dye. A peak at 381.4 nm ascribed to the dimeric form of CR dye was also blue shifted. The UV–Visible spectrum of CR dye before and after hybrid formation in ethylene glycol medium was studied by Gultek [26]. Moreover, it is well separated. The fluorescence emission spectrum of the nanohybrid system exhibited a peak at 519 nm (Fig. S2, spectrum b) whereas, the excitation spectrum (excited at 358 nm) showed a peak at 548.8 nm (Fig. S2, spectrum c). The red shift in the peak with respect to spectrum c in Fig. S1 explained the surface functionalization of ferrite by CR dye. The red shift in the emission peak confirmed the extension of electronic clouds.

Figure 4 indicates the UV–Visible spectra of CR dye modified copolymer samples. By increasing the loading of Fe_3O_4/CR nanohybrid, the absorption at 515 nm was increased linearly. This declares that equal concentration of ECH unit was present in the copolymer. The appearance of an absorption peak at 515 nm confirmed the chemical modification of copolymer by CR dye. Figure 4b indicates plots of log(weight of hybrid) vs. log(Abs.). The absorbance value was measured at 515 nm. The slope value of the curve was taken from the linear region which confirmed the order of the chemical modification reaction. The slope value was determined as 0.80. It means that 1.0 mol of CR dye is required to modify 1 mol of ECH units present in the PECH.

Figure 5 indicates the fluorescence emission spectra of copolymer samples structurally modified by CR dye at different loadings. The spectra exhibited one strong emission peak at 517 nm. By increasing the loading of Fe_3O_4/CR nanohybrid counterpart from 0.10 to 0.50 g, the FEI value of CR dye was increased. The rate of chemical modification based on the fluorescence emission value is shown in Fig. 5. The order of chemical structure modification of the copolymer by Fe_3O_4/CR nanohybrid counterpart can be determined using fluorescence emission spectroscopy. The plot of log (weight of hybrid) vs. log(FEI) is shown

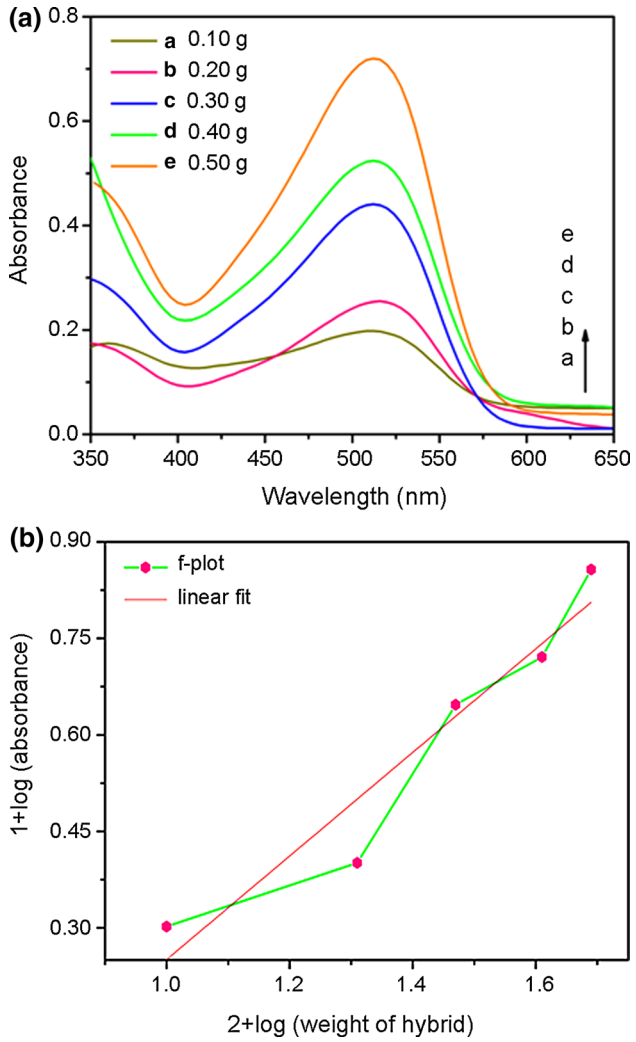

Fig. 4 **a** UV–Visible spectra of MA–PECH–PMMA copolymer samples at *a* 0.10, *b* 0.20, *c* 0.30, *d* 0.40, and *e* 0.50 g loadings of Fe_3O_4/CR nanohybrid system and **b** plot of log (weight of Fe_3O_4/CR) vs. log (Abs)

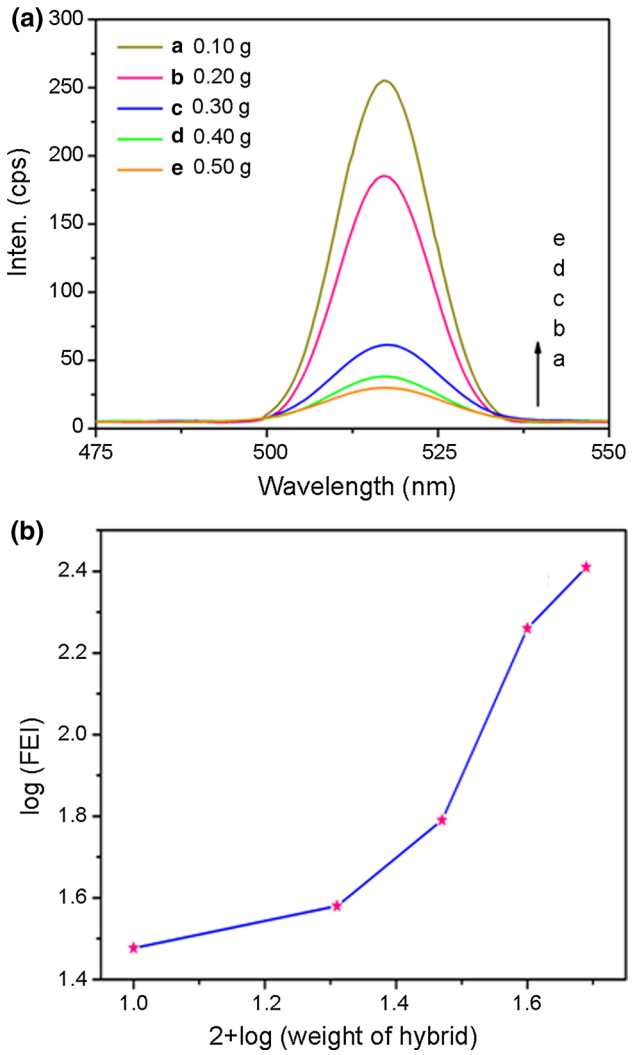

Fig. 5 **a** Fluorescence emission spectra of MA–PECH–PMMA copolymer samples at *a* 0.10, *b* 0.20, *c* 0.30, *d* 0.40, and *e* 0.50 g loadings of Fe_3O_4/CR nanohybrid system and **b** plot of log (weight of Fe_3O_4/CR) vs. log (FEI)

in Fig. 5b. It is interesting to note that while increasing the Fe_3O_4/CR nanohybrid loading, FEI value was also increased proportionally [33].

The slope value of the curve in Fig. 5b was determined as 1.07. It means that 1.07 mol of CR dye (includes the experimental error) is required for the structural modification of 1 mol of ECH units present in the PECH units. Since CR dye contains two amino groups, during the structural modification, it may bind with the copolymer in more than one site. The interaction may occur through an amino group (or) through the $–SO_3Na$ group of the CR dye. If amino groups interact with ECH units, there will be liberation of 1 mol of HCl. If $–SO_3Na$ groups interact with ECH units, 1 mol of NaCl is removed and facilitates the structural modification process. Both the absorbance and emission spectra confirmed that 1 mol of CR dye is required to modify 1 mol of the ECH units of the copolymer.

GPC analysis

The copolymer formation was further confirmed by molecular weight determination. The copolymer made from ECH and MMA units have the M_w of 24,154.3 g/mol and M_n of 17,010.7. The polydispersity Index (PDI) was determined as 1.41 and this confirmed the absence of cross-linking or branching. The M_w has also confirmed the copolymer formation. The GPC of the copolymer is shown in Fig. 6a. The molecular weight of PMMA synthesized in the presence

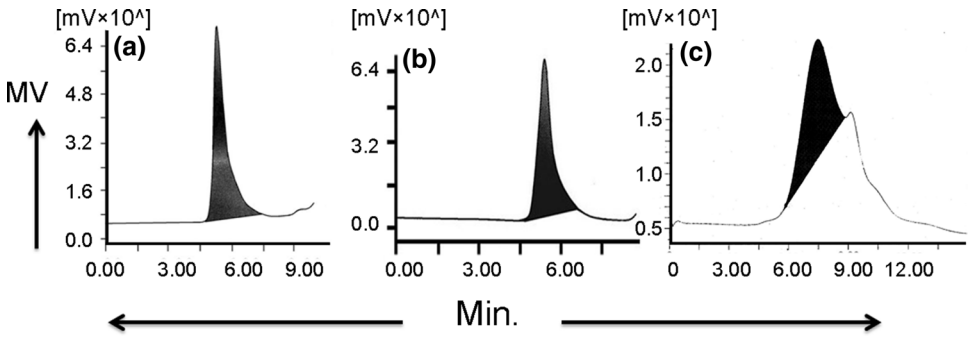

Fig. 6 GPC traces of **a** MA–PECH–PMMA, **b** MA–PECH–PMMA copolymer loaded with 0.30 g Fe_3O_4/CR nanohybrid system and **c** MA–PECH copolymer sample

of clay was thoroughly explained by Zhao et al. [40]. Our result coincides with their findings.

Figure 6b indicates the GPC of the CR-grafted copolymer. The –Cl atoms of ECH units present in the copolymer were replaced by the amino groups of the CR dye with the evolution of HCl as a by-product. After grafting with 0.3 g Fe_3O_4/CR nanohybrid system, the system exhibited the M_w, M_n and PDI values as 28,540.7 g/mol, 23,417.5, and 1.22, respectively. The increase in molecular weight after grafting reaction confirmed the incorporation of CR units into the backbone of PECH through the replacement of –Cl atoms.

Even after the chemical grafting reaction, the molecular weight of the copolymer was narrowed. It means that the reaction was occurred without any cross-linking reaction. The CR contains two amino groups which may act as bridging units between two copolymer chains. After the chemical grafting reaction, the water insoluble ECH units were water soluble and showed fluorescence property and processability. For the sake of convenience, the GPC trace of MA–PECH system is given in Fig. 6c and the M_w, M_n, and PDI values were determined as 6142.1 g/mol, 4067.5, and 1.51, respectively. The M_w of MA–PECH was lower than those of the MA–PECH–PMMA and Fe_3O_4/CR nanohybrid-grafted MA–PECH–PMMA system. The increase in molecular weight confirmed the copolymer formation and Fe_3O_4/CR grafting reaction onto copolymer backbone.

DSC analysis

The DSC analysis gives an idea about the thermal phase transition behavior of the polymers. The DSC thermogram of the copolymer is shown as curve a in Fig. 7. The thermogram did not show any endothermic or exothermic peaks corresponding to T_g and T_m values. The DSC thermograms of copolymer after the chemical modification with Fe_3O_4/CR nanohybrid system are represented as curves b–f in Fig. 7.

Since PMMA is an amorphous polymer, after copolymerizing with PECH, the crystallinity of the copolymer was suppressed further. But after the structural modification

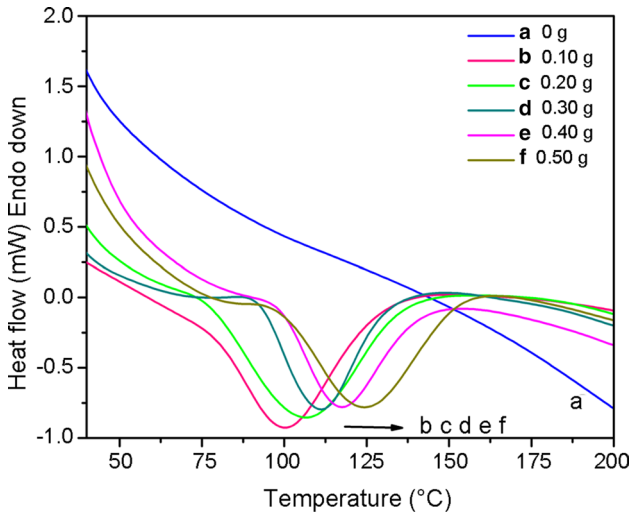

Fig. 7 DSC thermograms of MA–PECH–PMMA copolymer samples at *a* 0, *b* 0.10, *c* 0.20, *d* 0.30, *e* 0.40, and *f* 0.50 g loadings of Fe_3O_4/CR nanohybrid system

with CR dye again, the peak corresponding to the T_g of PMMA segments was appeared. The resin nature of PECH does not give any melt transition peak. While increasing the loading of Fe_3O_4/CR nanohybrid system, the T_m of PMMA was increased linearly from 100.1 to 123.7 °C. This is due to the presence of phenyl ring in the dye molecules which correspondingly increased the rigidity of the structure. As a result of increase in rigidity, the glass transition temperature was also increased. The important point noted here is while increasing the loading of Fe_3O_4/CR nanohybrid counterpart, the energy required for glass transition was reduced (i.e.,) the crystallinity of PMMA was indirectly reduced due to the random grafting.

Aldosari et al. [41] reported the T_g of neat PMMA as 117 °C. In the present investigation, the T_g value was initially found to be 100.1 °C, and by increasing the loading of nanohybrid counterpart, only T_g of PMMA was increased. After the grafting reaction or structural modification of the copolymer, T_g was higher than that of the above-mentioned literature value.

Thermogravimetric analysis

The thermal stabilities of the copolymer before and after structural modification with CR dye are exhibited in Fig. 8. The copolymer (Fig. 8, curve a) exhibited a three-step degradation process. The first minor weight loss around 107 °C was due to the removal of moisture and water molecules. The second minor weight loss around 250 °C was due to the breaking of ether linkages present in the PECH units. The third major weight loss around 410 °C corresponded to the degradation of the PMMA units with the evolution of CO_2. After the complete degradation, the copolymer showed a weight residue of 3.3 %. The copolymer after the structural modification with Fe_3O_4/CR nanohybrid system exhibited a three-step degradation process (Fig. 8, curves b–f). As usual, the first minor weight loss at 103 °C was associated with the removal of moisture and water molecules. The second weight loss around 360 °C could be explained on the basis of PMMA structural degradation with the simultaneous degradation of PECH units. The third minor weight loss around 442 °C was due to the breaking of CR dye molecules with the evolution of SO_2. Two interesting points were noted from the TGA thermogram. (i) By increasing the loading of Fe_3O_4/CR nanohybrid system from 0.10 to 0.50 g, the percentage weight residue around 500 °C was also increased from 44 to 66 %, respectively. (ii) By increasing the loading of Fe_3O_4/CR nanohybrid counterpart, the moisture as well as water absorption was also increased. For example, the 0.5 g Fe_3O_4/CR nanohybrid-modified copolymer exhibited considerable weight loss around 103 °C corresponding to the removal of moisture and physisorbed water molecules. On thorough analysis, one can come to a conclusion that after the structural modification of the copolymer with Fe_3O_4/CR nanohybrid system, thermal stability of the polymer was increased. Zhang et al. [42] reported that the T_d of PMMA varied from 360 to 420 °C. In the present investigation, the T_d value was reported as 360 °C. Hence our report is matched with the Zhang et al. [42] report.

FESEM analysis

Figure 9 indicates the FESEM micrographs of copolymer before and after the structural modification with ferrite/CR nanohybrid system. Figure 9a confirms the spherical morphology of the PMMA particles with a size of approximately 5 µm. Figure 9b shows the magnified micrograph of the same sample. The micrograph shows the agglomerated spherical morphology with some micro plates. The micro plates are formed as a result of the interface region between the PECH and PMMA. Here the PECH segments are acting as a hydrophilic soft segment, whereas

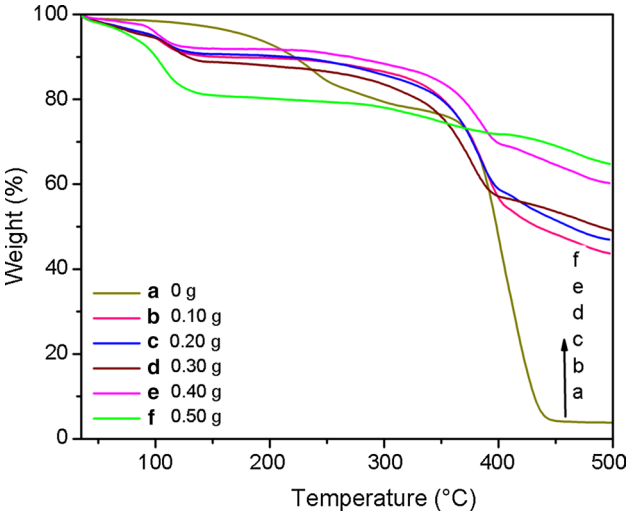

Fig. 8 TGA thermograms of MA–PECH–PMMA copolymer samples at *a* 0, *b* 0.10, *c* 0.20, *d* 0.30, *e* 0.40, and *f* 0.50 g loadings of Fe_3O_4/CR nanohybrid system

the PMMA segments are acting as hydrophobic hard segments. The interface regions between the hydrophilic and hydrophobic segments were compressed and resulting in the plate-shaped structure. Figure 9c represents the FESEM micrograph of Fe_3O_4/CR nanohybrid-modified copolymer. Amazingly, it is seen a gel-like morphology after the structural modification with Fe_3O_4/CR nanohybrid system. The size of microvoids was determined as ~2 µm. This type of surface morphology was very much useful in the drug delivery application because the micro-sized drugs can be easily accommodated in the microvoids. Once pH or temperature varied automatically, the drugs expelled out from the microvoids. Based on this concept, only the poly(caprolactone) (PCL) is acting as an efficient drug releasing material in the bio-medical field. Again, the micro voids are responsible for the efficient release of drugs.

Recently, our research team has reported about the presence of microvoids on the PCL backbone [34, 38]. Figure 9d indicates the magnified micrograph of the gel. Here, it can be seen a plate-like structure between the microvoids. Again, this is due to the suppressed spherical morphology of PMMA present in the interface region. This microplate can act as a wall, which can avoid the agglomeration of drug during the drug-loading process. It means that gel wall-like surface morphology can lead to the sustainable drug delivery.

Moreover, in the present investigation the ferrite nanoparticles were added as a hybrid and the same can control the drug delivery process with the targeted one. The spherical morphology of PMMA has been already reported by Zhao et al. [40]. Here also we get the same results.

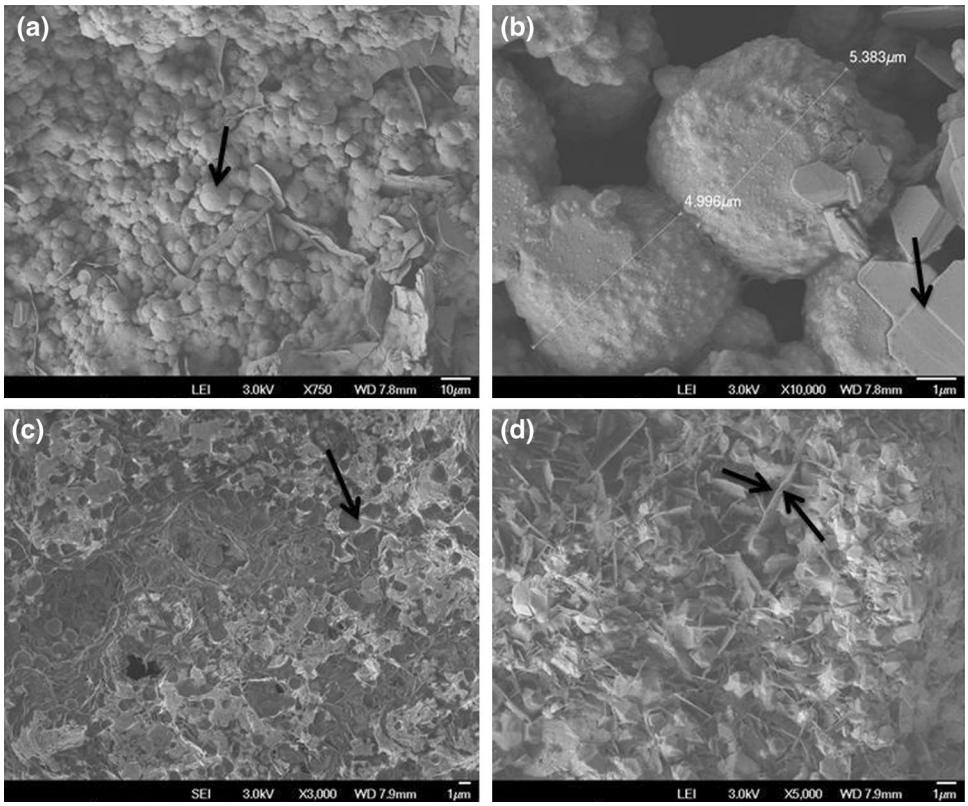

Fig. 9 FESEM micrographs of **a**, **b** MA–PECH–PMMA copolymer and **c**, **d** MA–PECH–PMMA copolymer loaded with 0.30 g Fe_3O_4/CR nanohybrid system at two different magnifications

VSM analysis

Figure S3 indicates the VSM loop of Fe_3O_4 before and after decoration and encapsulation. The magnetization value of pristine magnetite (Fig. S3a) was determined as 55.48 emu/g, whereas the nanohybrid system (Fig. S3b) shows the magnetization value of 50.89 emu/g. The decrease in magnetization value was due to the decoration or hybridization effects. The 0.30 g Fe_3O_4/CR nanohybrid-grafted MA–PECH–PMMA system (Fig. S3c) shows the magnetization value of 25.21 emu/g. The sudden decrease in magnetization value is explained on the basis of encapsulation effect. The Fe_3O_4 was encapsulated by a coil like form of the copolymer and hence decrease in the magnetization value. The polymer encapsulated Fe_3O_4 exhibited a lower magnetization value [43].

HRTEM study

The size of Fe_3O_4/CR nanohybrid system was determined with the help of HRTEM (JEM-200 CX, USA) instrument. Figure 10 indicates the HRTEM micrograph of the Fe_3O_4 nanoparticles. The size of Fe_3O_4 nanoparticles was varied between 10 and 50 nm with a distorted spherical morphology. The distorted morphology of the Fe_3O_4 nanoparticles was due to the agglomeration effect. The HRTEM of ferrite has been reported in the literature, as well [44, 45].

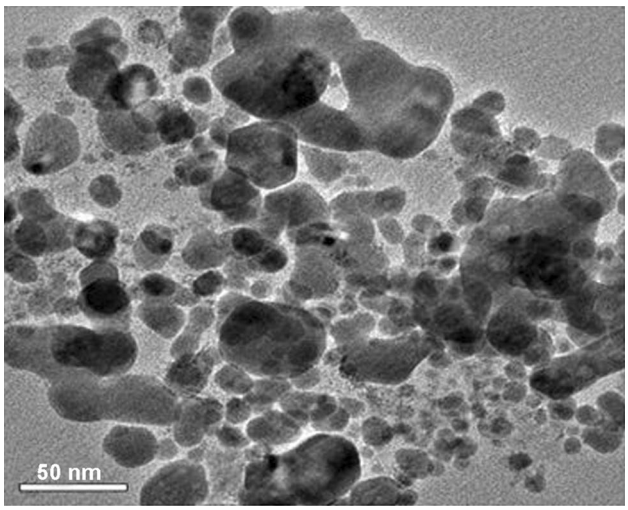

Fig. 10 HRTEM micrograph of Fe_3O_4/CR nanohybrid system

Conclusion

In this study synthesis and characterization, a fluorescent material by way of structural modification of PECH copolymer with CR/Fe_3O_4 nanohybrid system are presented. The FTIR spectrum confirmed the presence of Fe–O stretching vibration in the copolymer around 550 cm^{-1}. The shift in

the peak positions (both in UV–Visible and fluorescence emission spectra) confirmed the structural modification of copolymer by the nanohybrid system. The increase in T_g and T_d values of the structurally modified copolymer was confirmed by DSC and TGA thermograms, respectively, when increased the loading of nanohybrid counterpart. The hydrogel-like morphology also confirmed the structural modification of the copolymer by the hybrid system. The weight average molecular weight of the structurally modified copolymer was higher than that of the non-modified copolymer. The VSM value of the pristine Fe_3O_4 (55.48 emu/g) was higher than those of the hybrid (50.89 emu/g) and the copolymer nanocomposite (25.21 emu/g) systems. The HRTEM confirmed the size of the ferrite particles as 10–50 nm. The present investigation was focused on the preparation of a material for bio-imaging and targeted drug delivery applications.

Acknowledgments We sincerely acknowledged Mrs. G. Vijayalakshmi, Assistant Professor of English Department for her valuable help during the manuscript preparation.

References

1. Knop K, Hoogenbeom R, Fischer D, Schubert US (2010) PEG in drug delivery: Pros and Cons as well as potential alternatives. Angew Chem Int Ed 49:6288–6308
2. Armand M (1990) Polymers with ionic conductivity. Adv Mater 2:278–286
3. Liu J, Sun J, Shen Z (1994) The polymerization of ECH with $Nd(i\text{-}OPr)_3$–Al $(i\text{-}Bu)_3$ system. Chin J Polym Sci 12:153–156
4. Nogueira AF, Spinace MAS, Gazotti WA, Girotto EM, de Paoli MA (2001) Poly(ethylene oxide-co-epichlorohydrin)/NaI: a promising polymer electrolyte for photoelectrochemical cells. Solid State Ionics 140:327–335
5. Bhosale SV, Rasool MA, Reina JA, Giamberini M (2013) New hybrid crystal columnar poly(epichlorohydrin-co-ethyleneoxide) derivatives leading biomimetic ion channels. Polym Eng Sci 53:159–167
6. Callau L, Reina JA, Manteaon A, Tessier M, Sparsky N (1999) Vinyl terminated side chain liquid crystalline derivatives containing biphenyl naphthalene mesogenic moieties. Macromolecules 32:7790–7797
7. Nouailhas H, Aouf C, Boutevin B, Fulcrand H, Guerneve CL, Caillol S (2011) Synthesis and preparation of bio based epoxy resins. Part 1. Glycidylation of flavonoids by epichlorohydrin. J Polym Sci Polym Chem 49:2261–2270
8. Alupei IC, Popa M, Abadie MJM, Hamcerencu M (2002) Super absorbent hydrogels based on xanthan and PVA—the study of the swelling properties. Eur Polym J 38:2313–2320
9. Han X, Shanks RA, Pavel D (2005) The synthesis and thermal properties of poly(epichlorohydrin) side chain liquid crystal polymers. Eur Polym J 41:984–991
10. Callau L, Reina JA, Mantecon A (2002) Cross linking of vinyl terminated side chain liquid crystalline polyethers using low molecular weight analogous mesogenic esters as reactive diluents. Polymer 43:6391–6396
11. Buruaga L, Pomposo JA (2011) Metal free PMMA nanoparticles by enamine click chemistry at room temperature. Polymers 3:1673–1683
12. Pathmamanoharan C, Slob C, Lekkerkerker HNW (1989) Preparation of poly(methylmethacrylate) lattices in non-polar media. Coilloid Polym Sci 267:448–450
13. Parzuchowski PG, Frost MC, Meyerhoff ME (2002) Synthesis and characterization based nitric oxide donors. J Am Chem Soc 124:12182–12191
14. Costache MC, Wang D, Heidecker MJ, Manias E, Wilkie CA (2006) The thermal degradation of PMMA nanocomposites with montmorillonite, layered double hydroxides and carbon nanotubes. Polym Adv Technol 17:272–280
15. Katsikas L, Avramovic M, Popovic IG, Cortes RDB, Milovanovic M, Kalagasidis-Krusic MT (2008) The thermal stability of PMMA by RAFT polymerisation. J Serb Chem Soc 73C:915–921
16. Bicak N, Gazi M, Tunca U, Kucukkaya I (2004) Utility of atom transfer radical polymerization for the preparation of PMMA beads in an aqueous suspension. J Polym Sci Polym Chem 42:1362–1366
17. Hammudi ZT, Nugay N, Nugay T (2004) Anionic polymerization of methyl methacrylate as promoted by a N-butyl lithium-pyridazine-polyether alkoxide based complex initiator system. Turk J Chem 28:387–394
18. Ahmad S, Ahmad S, Agnihotry SA (2007) Synthesis and characterization of in situ prepared PMMA nanocomposites. Bull Mater Sci 1:31–35
19. Nikolaidis AK, Achilias DS, Karayannidis GP (2011) Synthesis and characterization of PMMA/organo modified montmorillonite nanocomposites prepared by in situ bulk polymerization. Ind Eng Chem Res 50:571–579
20. Klein SM, Manoharan VN, Pine DJ, Lange FF (2003) Preparation of monodisperse PMMA microsphere in non-polar solvents by dispersion polymerisation with a macromonomeric stabilizer. Colloid Polym Sci 282:7–13
21. Gong S, Ma H, Wan X (2006) Atom transfer radical polymerization of methyl methacrylate induced by an initiator derived from an ionic liquid. Polym Int 55:1420–1425
22. Tonga JD, Leclere PH, Doneux C, Bredas JL, Lazzaroni R, Jerome R (2000) Synthesis and bulk properties of poly(methyl methacrylate)-b-poly(isooctyl acrylate)-b-poly(methyl methacrylate). Polymer 41:4617–4624
23. Nájera MA, Elizalde LE, Vázquez Y, Gdl Santos (2009) Synthesis of random copolymers poly(methylmethacrylate-*co*-azo monomer) by ATRP-AGET. Macromol Symp 283–284:51–55
24. Tang T, Castelletto V, Parras P, Hamley IW, King SM, Roy D, Perrier S, Hoogenboom R, Schubert US (2006) Thermoresponsive poly(methyl methacrylate)-block-poly(*N*-isopropylacrylamide) block copolymers synthesized by RAFT polymerization micellization and gelation. Macromol Chem Phys 207:1718–1726
25. Król P, Chmielarz P (2013) Synthesis of PMMA-*b*-PU-*b*-PMMA tri-block copolymers through ARGET ATRP in the presence of air. Express Polym Lett 7:249–260
26. Gultek A (2010) Synthesis and characterization of hybrid congo red from chloro-functionalized silsesquioxanes. Turk J Chem 34:437–445
27. Dafare S, Deshpande PS, Bhavsar RS (2013) Photocatalytic degradation of congo red dye on combustion synthesised Fe_2O_3. Ind J Chem Technol 20:406–410
28. Movahedi M, Mahjoub AR, Janitabar S (2009) Photodegradation of congo red in aqueous solution on ZnO as an alternative catalyst to TiO_2. J Iran Chem Soc 6:570–577

29. Hu S, Yan P, Maslov K, Lee JM, Wang LV (2009) Intra vital imaging of amyloid plaques in a transgenic mouse model using optical resolution photoacoustic micros. Opt Lett 34:3899–3901
30. Mathur T, Singhal S, Khan S, Upadhyay DJ, Fatma T, Rattan A (2006) Detection of biofilm formation among the clinical isolates of staphylococci: an evaluation of three different screening methods. Indian J Med Microbiol 24:25–29
31. Kumar P, Selvi SS, Govindaraju M (2012) In vitro anti-biofilm and anti-bacterial activity of *Junceella juncea* for its biomedical application. Asian Pac J Trop Biomed 2:930–935
32. Li X, Qian Y, Liu T, Hu X, Zhang G, You Y, Liu S (2011) Amphiphilic multiarm star block copolymer-based multifunctional unimolecular micelles for cancer targeted drug delivery and MR imaging. Biomaterials 32:6595–6605
33. Meenarathi B, Palanikumar S, Kannammal L, Anbarasan R (2015) Synthesis, characterization and catalytic activity of Ag-acidfuchsin nanohybrid system towards the ring opening polymerization of ε-caprolactone. Spectrochim Acta A Mol Biomol Spectrosc 135:93–100
34. Murugesan A, Meenarathi B, Palanikumar S, Kannammal L, Anbarasan R (2014) Synthesis, characterization and drug delivery activity of poly(anthranilic acid) based triblock copolymer. Synth Met 189:143–151
35. Bernogozzi I, Torrengo S, Minati L, Ferrari M, Chiappini A, Armellini C, Toniutti L, Lunelli L, Speranza G (2012) Synthesis and characterization of PMMA-based superhydrophobic surfaces. Colloid Polym Sci 290:315–322
36. Fang FF, Kim JH, Choi HJ, Kim CA (2009) Synthesis and electro rheological response of nanosized laponite stabilized PMMA. Colloid Polym Sci 287:745–749
37. Meenarathi B, Kannammal L, Palanikumar S, Anbarasan R (2014) Synthesis and characterization of Fe_3O_4-acidfuchsin tagged poly(ε-caprolactone) nanocomposites. Mater Res Exp 1:1–16
38. Meenarathi Chen HH, Chen PH, Anbarasan R (2013) NIR dye functionalized dye MWCNT as an effective initiator for the ring opening polymerization of ε-Caprolactone. J Polym Res 20:118–130
39. Palanikumar S, Siva P, Meenarathi B, Kannammal L, Anbarasan R (2014) Effect of Fe_3O_4 on the sedimentation and structure-property relationship of starch under different pHs. Int J Biol Macromol 67:91–98
40. Zhao Q, Samulski ET (2006) A comparative study of PMMA and poly(styrene)/clay nanocomposites prepared in super critical CO_2. Polymer 47:663–671
41. Aldosari MA, Othman AA, Alsharaeh EH (2013) Synthesis and characterization of the in situ bulk polymerization of poly(methylmethacrylate) containing graphene sheets using microwave irradiation. Molecules 18:3152–3167
42. Zhang B, Blum FD (2002) Thermogravimetric studies of poly(methylmethacrylate) on silica. Polym Prepr 43:484–485
43. Aouak T, Deraz NM, Alarifi AS (2013) Synthesis, non-isothermal crystallization and magnetic properties of $Co_{0.25}Zn_{0.25}Fe_2O_4$/poly(ethylene-*co*-vinylalcohol) nanocomposite. Bull Mater Sci 36:417–427
44. Singh JP, Dixit G, Negi P, Sirvastava RC, Negi P, Agrawal HM, Kumar R (2013) HRTEM and FTIR investigation of nanosized Zinc ferrite irradiated with 100 MeV oxygen ions. Spectrochim Acta Part A 107:326–333
45. Mahdavinia GR, Iravani S, Zoroufi S, Hosseinzadeh H (2014) Magnetic and K^+ cross linked kappa carregeenan nanocomposite beads and adsorption of crystal violet. Iran Polym J 23:335–344